MEMS Dual-mode Electrostatically Actuated Micromirror

Xingguo Xiong
Department of Electrical Engineering
University of Bridgeport
Bridgeport, CT 06604
xxiong@bridgeport.edu

Hanyu Xie
Department of Electrical Engineering
University of Bridgeport
Bridgeport, CT 06604
hanyuxie@my.bridgeport.edu

***Abstract* — Micromirrors based on MEMS (Micro-electromechanical Systems) technology have been widely used in light display, optical communication and other applications. In this paper, an electrostatically actuated dual-mode micromirror device is proposed. Folded beam structure is used for piston movement and straight beams are used for torsional movement. Two switches connected to bottom aluminum driving electrodes are used to control the working mode of the micromirror. Depending on the need, it can be activated to work in either piston or torsional mode. The working principle of the micromirror is analyzed. Equations are derived to predict the performance of the micromirror in both piston and torsional modes. ANSYS simulation is used to verify the vibrational modes of the dual-mode micromirror. The proposed micromirror integrates both piston and torsional functions in a single device, leading to more flexibility and better efficiency.**

Keywords — Microelectromechanical Systems (MEMS), Micromirror, Dual-mode, Piston Micromirror, Torsional Micromirror.

I. INTRODUCTION

Microelectromechanical Systems (MEMS) technology refers to devices and systems in micro scale that combines electrical and mechanical components and are fabricated with micromachining techniques. MEMS devices generally have the feature size in the range of 1 micron to 1 millimeter (1μm~1mm). Due to such small size, MEMS devices have the advantages of low weight, low cost, low energy consumption, quick response time, high resolution and high sensitivity. Various MEMS devices have been developed and commercialized, such as MEMS accelerometers, gyroscopes, micropumps, microgears, microresonators, etc. Micromirrors are important optical actuators in MEMS family. Generally micromirrors are considered as tiny mirrors which are controlled using electrostatic force or other actuation techniques. Micromirrors are used to reflect incident light to an expected direction by moving the mirror plate, so that the phase and/or the amplitude of the incident light can be modulated. Micromirrors have been widely used since the Digital Micromirror Devices (DMD) were invented by Texas Instruments in 1987 and used for video projection [1]. Nowadays Micromirror devices have been utilized in numerous optical systems including micro displays, optical cross-connects for telecommunication networks, free-space optical communication links and optical coherence tomography systems.

According to their working modes, MEMS micromirrors [2]-[5] can be divided into two categories: piston micromirrors and torsional micromirrors. Piston micromirrors move perpendicular to the substrate. They can be used to modify the phase of incident light. Torsional micromirrors tilt along certain axis, hence change the direction of incident light. To offer more functionalities, dual-mode micromirrors which can work in either piston or torsional modes are needed. Various dual-mode micromirrors have been reported [6]-[11]. In [8], a dual-mode micromirror based on stacked vertical comb drive actuator for optical phased array application is reported. It utilizes two sets of static top layer comb teeth and two sets of static bottom layer comb teeth to activate the micromirror to work in piston or torsional mode. The advantage of using comb actuator is that it allows large deflections at relatively low driving voltage with continuous stable control over the full range of motion. In [9], a one-dimensional spatial light phase modulator (SLPM) consisting of a micromirror array on SOI wafer and ITO (Indium Tin Oxide) electrodes on a glass substrate is reported. Each micromirror in the array can be actuated to work in bi-derectional single-axis rotation as well as up-and-down piston movement. Due to its differential actuation structure, the micromirror can work in tilt mode, piston mode, and tilt-and-piston mode. In [10], an electrothermally actuated single-crystal-silicon (SCS) dual-mode micromirror for large bi-directional scanning is reported. Due to its electrothermal actuation, it can perform large bi-directional scans as well as large piston displacement with relatively low driving voltage (less than 6Vdc). In [11], an aluminum bi-functional spatial light modulator was reported. It utilizes electrostatic actuation with two switches to control the micromirror to work either in piston or torsional mode. Four folded beams are used for piston movement and two straight beams are used for torsional movement. The micromirror was proposed to be

978-1-4799-5233-5/14/$31.00 ©2014 IEEE

fabricated with surface-micromachining using thick-photoresist sacrificial layer technique. In this paper, an electrostatically-actuated micromirror with different folded-beam structure is reported.

II. MICROMIRROR DESIGN AND WORKING PRINCIPLE

The structure diagram of the MEMS dual-mode micromirror device is shown in Fig. 1. Aluminum is used as the structure material of the micromirror for its excellent light reflectivity. The optical reflectivity of smooth aluminum surfaces to light is more than 90% for light wavelength of 0.9μm~12.0μm [12]. As show in the figure, two aluminum mirror plates are supported by two torsional beams and four folded beams on top of silicon substrate. Between the aluminum mirror and the silicon substrate, there is a thin layer of silicon dioxide (SiO_2) for insulation purpose. Below each mirror plate, there is an aluminum bottom electrode on top of substrate for electrostatic actuation. The floating (movable) parts are in light gray color and the two anchors are in dark color. Folded beam structure is used for piston mode because it can increase the effective length of the beam and lead to small spring constant, hence lowering the required driving voltage. Unlike Digital Micromirror Device (DMD) [1] by Texas Instruments, this micromirror uses only a single layer of structure material. This results in simple fabrication process. However, the filling ratio of the mirror is less than 100%.

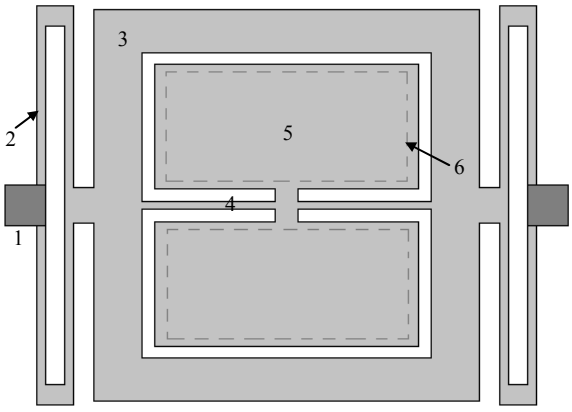

Figure 1. Structure design of the MEMS dual-mode electrostatic micromirror: 1. Anchor (×2), 2. Piston folded beam (×4), 3. Mirror frame, 4. Torsinal beam, 5. Mirror plate (×2), 6. Bottom Al actuation electrode (×2).

The working principle of the MEMS dual-mode micromirror is shown in Fig. 2. In order to make it easy for illustration, the folded beams are plotted at the left and right sides of both mirror plates. This is not the actual cross sectional view of the device, but it makes our explanation easier. The proposed dual-mode micromirror can work in two modes: piston mode and torsional mode. Driving voltage V_d is applied between the mirror plates and the bottom aluminum electrodes via two switches (sw1 and sw2).

As shown in Fig. 2(a), in Piston mode, both switches (sw1 and sw2) are turned on. Driving voltage V_d is applied between the mirror plates and both bottom Al electrodes. As a result, both mirror plates experience electrostatic forces F_e toward the bottom. The total electrostatic forces cause both mirror plates to move down. The total displacement of the mirror plates is equal to the sum of the bending of four folded beams, as well as the bending of the torsional beams. This is the piston mode of the micromirror.

As shown in Fig. 2(b), in torsional mode, only one switch (sw1 or sw2) is turned on. As a result, only one of the two mirror plates experiences electrostatic force toward the bottom. In the figure, we show that the sw1 is off and sw2 is on. The right mirror plate experiences electrostatic force but the left mirror plate does not. This results in a net torque around the torsional beam. Hence the mirror plates rotate (tilt) around the torsional beam, and the micromirror works in torsional mode.

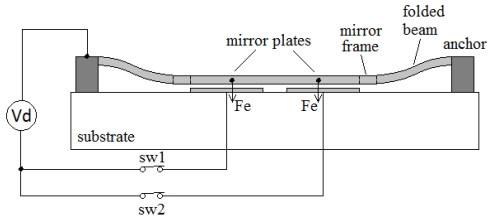

(a). piston mode of the micromirror

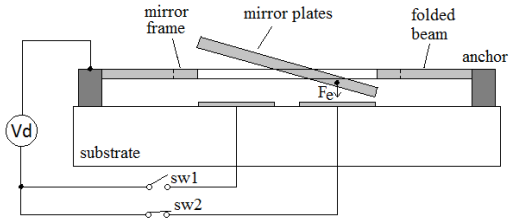

(b). torsional mode of the micromirror

Figure 2. The piston and torsional modes of the MEMS micromirror

III. THEORETICAL ANALYSIS OF THE MICROMIRROR

Theoretical analysis is important to guide the device design. To help the discussion, some key design parameters of the micromirror are defined as below and shown in Fig. 3. Assume the beam width/length of first section of folded beam are W_1 and L_1, the width/length of second section of the folded beam are W_2 and L_2. The width and length of each section of torsional beams are W_3 and L_3. The width and length of the mirror frame are W_f and L_f respectively. The length of aluminum bottom electrode is L_e. The distance between two outer edges of mirror plates is a. The gap between two bottom aluminum electrodes is a_1. The distance between two outer edges of bottom aluminum electrodes is a_2. The device thickness is t, and Young's modulus of aluminum material is E. The gap between mirror plates and bottom aluminum electrodes is h.

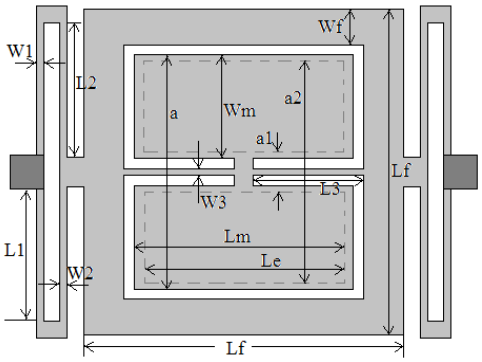

Figure 3. Design parameters of the micromirror

3.1 Piston mode of the micromirror

In piston mode, both switches are turned on and electrostatic forces are applied to both mirror plates. As a result, the mirror plates move down perpendicular to the substrate. The majority of the displacement comes from the four folded beams. The torsional beams also bends under electrostatic force and contributes to the total bending displacement. Furthermore, the gravity force of the mirror frame and the mirror plates also causes small bending of the folded beams and the torsional beams. To be more accurate, this effect should also be considered.

Each folded beam consists of two sections connected in series, and the four folded beams are connected in parallel. The bending of the folded beams can be treated as simplified spring-mass model. The equivalent spring constants of two section of folded beam can be calculated as

$$K_{b1} = \frac{12EI_1}{L_1^3} = \frac{EW_1t^3}{L_1^3} \tag{1}$$

$$K_{b2} = \frac{12EI_2}{L_2^3} = \frac{EW_2t^3}{L_2^3} \tag{2}$$

where E is E is the Young's modulus of aluminum material, $E_{Al}=7\times10^9 Pa$. I_1 and I2 are the inertial momentum of the beam sections:

$$I_1 = \frac{1}{12}W_1t^3 \tag{3}$$

$$I_2 = \frac{1}{12}W_2t^3 \tag{4}$$

Since two beam sections of folded beam are connected in series, the total spring constant of one folded beam is

$$K_{fold1} = \frac{K_{b1}\cdot K_{b2}}{(K_{b1}+K_{b2})} \tag{5}$$

The four folded beams are connected in parallel. Thus the total spring constant of four folded beams is

$$K_{fold} = 4K_{fold1} = \frac{4K_{b1}\cdot K_{b2}}{(K_{b1}+K_{b2})} \tag{6}$$

The two sections of torsional beams also contribute to the bending displacement in piston mode. The equivalent spring constant of one section of torsional beam is

$$K_{b3} = \frac{12EI_3}{L_3^3} = \frac{EW_3t^3}{L_3^3} \tag{7}$$

where I_3 is the inertial momentum of one torsional beam section:

$$I_3 = \frac{1}{12}W_3t^3 \tag{8}$$

Both sections of torsional beams are connected in parallel. Thus the total spring constant of both torsional beams is

$$K_{tor} = 2K_{b3} = \frac{2EW_3t^3}{L_3^3} \tag{9}$$

In piston mode, the folded beams and torsional beams are connected in parallel to contribute to the total piston displacement of the micromirror. The total spring constant of the micromirror in piston mode is

$$K_{piston} = K_{fold} + K_{tor} = \frac{4K_{b1}\cdot K_{b2}}{(K_{b1}+K_{b2})} + 2K_{b3} \tag{10}$$

If the spring constant in piston mode is calculated, the corresponding resonant frequency of the micromirror in piston mode can be calculated as

$$f_{piston} = \frac{1}{2\pi}\sqrt{\frac{K_{piston}}{M}} \tag{11}$$

Where M includes the mass of mirror plates and the mirror frame. Resonant frequency is an important factor for the dynamic performance of micromirror.

In piston mode, when driving voltage V_d is applied, the electrostatic force causes mirror plates to move down. The electrostatic force and the gravity force of the mirrors and the frame are balanced by restoring force of folded beams and torsional beams. When all the forces come to equilibrium, the mirror plates move down with stable displacement of x. The gravity force of the mirror plates and frame is

$$F_m = \rho\cdot V\cdot g = \rho\left[2W_mL_m + 4W_f(L_f - W_f)\right]t\cdot g \tag{12}$$

where ρ is density of aluminum material ($\rho_{Al}=2.7\times10^3 kg/m^3$), g is gravity acceleration ($g=9.8 m/s^2$).

When the mirror plates move down by displacement x, the total electrostatic force applied on both mirror plates is

$$F_e = \frac{\varepsilon(a2-a1)L_eV_d^2}{2(h-x)^2} \tag{13}$$

In it, ε is dielectric constant of air.

The restoring force of the folded beams and torsional beams is

$$F_k = -K_{piston}\cdot x \tag{14}$$

When all the forces come to equilibrium, we have

$$F_e + F_m + F_k = 0 \tag{15}$$

That is

$$\frac{\varepsilon(a2-a1)L_eV_d^2}{2(h-x)^2} + \rho[2W_mL_m + 4(L_f - W_f)W_f]t\cdot g = K_{piston}\cdot x \tag{16}$$

Solving this equation, we can find out the stable displacement x of the micromirror in piston mode. The

third-order equation may give three solutions for x, however, only one solution within the range of $0<x<(1/3)h$ will be valid stable solution because it does not lead to pull-down effect.

We can also rewrite the equation to find out the required driving voltage V_d in order to achieve a certain displacement x as

$$V_d = \sqrt{\frac{2(h-x)^2\left\{K_{piston}\cdot x - \rho[2\,W_m L_m + 4(L_f - W_f)W_f]t\cdot g\right\}}{\varepsilon(a2-a1)L_e}} \quad (17)$$

Based on above equation, we can find out the required driving voltage for any displacement x. However, the displacement x cannot go beyond certain range. As we know, electrostatic force increase rapidly with displacement x. It approaches infinity as displacement x approaches capacitance gap h. Restoring force F_k only increases linearly with displacement x. As the displacement x continues to increase, the restoring force will not be able to balance the quick increase of electrostatic force. As a result, the mirror will continue to move down toward the substrate and eventually get stuck with the substrate. This is the so-called "pull-down effect" of piston micromirror. The pull-down threshold voltage V_{dmax} can be found by solving equation $(dV_d/dx)=0$.

3.2 Torsional mode analysis

In the torsional mode, either switch sw1 or sw2 is turned on. Driving voltage V_d is applied between one of the mirror plates and its bottom aluminum electrode. This results in torque and cause the mirror plates to tilt around the torsional beam. In order to reduce the tilting effect of the connector between folded beams and the mirror frame, we intentionally widen this portion of connector, as shown in Fig. 1. Thus we can treat this portion of connector as rigid body and non-deformable. The majority of the tilting comes from the two torsional beams. The torsional stiffness S_3 of one section of torsional beam can be calculated as

$$S_3 = \frac{GI_3}{L_3} \quad (18)$$

where G is the shear modulus of aluminum material, $G_{Al}=26GPa$. I_3 is the inertial momentum of one section of torsonal beam. In case $W_3>t$, it can be calculated as [13]:

$$I_3 = t^3 W_3\left[\frac{1}{3} - 0.21\cdot\frac{t}{W_3}\cdot\left(1-\frac{t^4}{12W_3^4}\right)\right] \quad (19)$$

Two sections of torsional beams are connected in parallel. The total torsional stiffness of both torsional beams is

$$S_{tor} = 2S_3 = \frac{2GI_3}{L_3} \quad (20)$$

The rotation angle of mirror plates in torsional mode can be calculated by equilibrium equation [13]

$$M_e = S_t \cdot \theta \quad (21)$$

where M_e is the torsional moment of the electrostatic force, θ is the rotation angle of mirror plates. The electrostatic force is distributed force on the mirror plates. The total torsional torque of electrostatic force needs to be calculated using integral. According to [13], define normalized rotation angle Θ as:

$$\Theta = \theta / \theta_{\max} \quad (22)$$

where $\theta_{\max} = \tan^{-1}(2h/a)$ is the nominal maximum allowed torsional angle, that is, the maximum torsional angle when the edge of the mirror plate touches the substrate. The relationship between the normalized rotation angle and the torsional driving voltage V_d can be expresses as [13]:

$$V_d = k_0\left[\frac{\Theta^3}{(1/(1-\beta\Theta)) - (1/(1-\alpha\Theta)) + \ln[(1-\beta\Theta)/(1-\alpha\Theta)]}\right]^{1/2} \quad (23)$$

where $\alpha = a1/a$, $\beta = a2/a$, k_0 is a constant defined as

$$k_0 = \left[\frac{2S_{tor}\theta_{\max}^3}{\varepsilon L_3}\right]^{1/2} \quad (24)$$

For given rotation angle θ, we can convert it into normalized rotation angle Θ. Based on above equation, the corresponding torsional driving voltage can be calculated.

Similar to piston mode, the torsional mode of micromirror also suffers from snap-down effect. That is, if the torsoinal angle exceeds a threshold value (snap-down angle θ_{snap}), the restoring force cannot balance the quick increase of the torque of the electrostatic force. Hence, the mirror plate will continue to tilt till finally the edge of mirror plate touches the substrate. The calculation of the threshold voltage for snap-down effect in torsional mode is complex. If the gap between aluminum electrodes can be ignored (i.e. a1=α=0), then the threshold snap-down driving voltage V_{d_snap} can be calculated as [13]

$$V_{d\_snap} = 0.6432 k_0 \beta^{-3/2} \quad (25)$$

The corresponding threshold snap-down angle θ_{snap} can be calculated by [13]

$$\theta_{snap} = \frac{0.4404\theta_{\max}}{\beta} \quad (26)$$

Once the rotation angle exceeds this snap-down angle ($\theta>\theta_{snap}$), mirror plates continue to tilt till finally the edge of mirror plate touches the substrate and the maximum allowed rotation angle ($\theta=\theta_{max}$) is achieved. For digital micromirror, we intentionally set the torsional angle to be larger than snap-down angle. That is, we intentionally utilize the snap-down effect of the torsional mirror for its digital operation.

IV. DEVICE DESIGN AND SIMULATION

Based on the theoretical analysis, a set of example optimized design parameters of the MEMS dual-mode micromirror are proposed. The structure design parameters of the micromirror are shown in Table 1. The corresponding performance parameters of the micromirror design (by hand calculation based on the theoretical equations) are listed in Table 2.

TABLE I. DESIGN PARAMETERS OF MICROMIRROR

Design Parameters	Values
Mirror plate (each) ($W_m \times L_m \times t$)	30×60×1μm
Thickness of mirror (t)	1μm
Piston beam section #1 ($W_1 \times L_1 \times t$)	2×88×1μm
Piston beam section #2 ($W_2 \times L_2 \times t$)	2×39×1μm
Torsional beam width (one section) ($W_3 \times L_3 \times t$)	2×64×1μm
Inner distance between two Al electrodes (a1)	6μm
Outer distance between two Al electrodes (a2)	66μm
Outer distance between mirror plates (a)	66μm
Gap between mirror and substrate (h)	4μm

TABLE II. PERFORMANCE PARAMETERS OF MICROMIRROR

Performance Parameters	Values
Piston mode nominal maximum displacement (h)	4μm
Piston mode pull-in displacement (x_{pull_in})	1.33μm
Piston mode pull-in voltage (V_{pull_in})	24.99V
Piston working frequency (f_{0p})	185.7kHz
Torsional mode nominal maximum rotation angle (θ_{max})	6.91°
Torsional mode snap-down angle (θ_{snap_down})	3.04°
Torsional mode snap-down voltage (V_{snap_down})	31.04V

Based on the theoretical analysis, the relationship between piston displacement of micromirror versus driving voltage is plotted in Fig. 4. As shown in Fig. 5, we can see that initially when the driving voltage V_d increases, the piston displacement *x* increases. However, once the driving voltage exceeds the threshold pull-down voltage (V_{pull_down}=24.99V), the piston displacement quickly increases to 4μm, which is the gap between the mirror plate and substrate. This indicates that the restoring force of the beams cannot balance the electrostatic force. As a result, the mirror continue to move till finally it touches the substrate. This is the pull-down effect of the micromirror in piston mode. To achieve controllable displacement of the micromirror in piston mode, we should maintain the driving voltage to be less than the threshold pull-in voltage (V_d<V_{pull_down}).

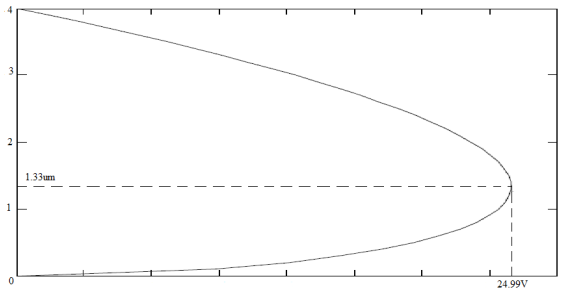

Figure 4. Piston displacement (Y-axis) versus driving voltage V_d (X-axis) of the micromirror

We can also plot the relationship between the torsional angle of the micromirror versus the driving voltage in torsional mode, as shown in Fig. 5. As we can see in the figure, the torsional angle initially increases with driving voltage V_d. However, once the driving voltage increases beyond a threshold value ($V_{snap\text{-}down}$=31.04V), the torsional angle θ quickly increases till finally it approaches the maximum allowed torsional angle (θ_{max}=6.91˚) so that the mirror edge touches the substrate. That is, the torque of restoring force cannot balance the quick increase of the torque of electrostatic force. Hence the snap-down effect occurs in the torsional mode. If the micromirror is used as digital mirror in torsional mode, we intentionally set the driving voltage to be larger than the snap-in voltage so that the micromirror tilts all the way left or right toward the substrate.

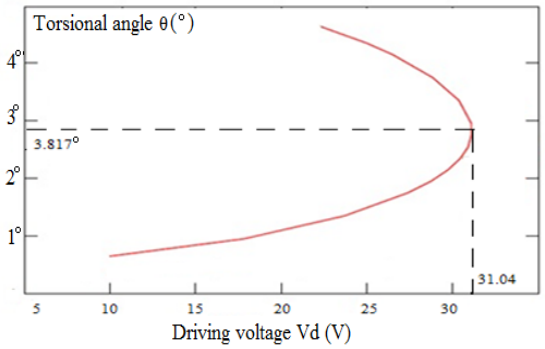

Figure 5. Torsional angle versus driving voltage V_d of the micromirror in torsional mode

In order to verify the function of the dual-mode MEMS micromirror, we use ANSYS FEM (Finite Element Method) to simulate the designed micromirror. ANSYS modal simulation is performed on the micromirror and the resonant frequencies of the first 10 vibrational modes of the micromirror are extracted, as shown in Fig. 6.

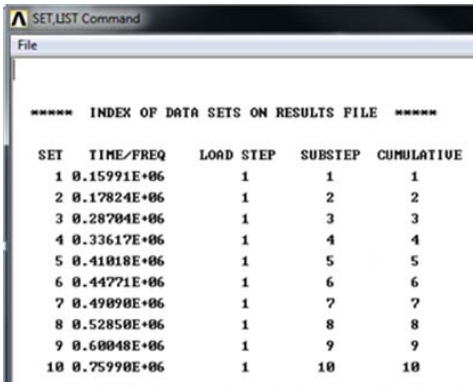

Figure 6. ANSYS simulation results of first 10 vibrational modes of micromirror

By observing the animation of each vibration modes, we identify that the first two vibrational modes are the working modes of the micromirror. In the first vibrational mode (see Fig. 7), the mirror plates move up and down perpendicular to the substrate with resonant frequency of f_0=159.91kHz. This is the piston mode of the micromirror. Using the simplified spring-mass model, the resonant frequency of the micromirror in piston mode was calculated as f_0=185.7kHz, which is close to the ANSYS simulation result with an relative error of 16.1%. ANSYS simulation

result is more accurate and trustworthy because hand calculation is based on simplified spring-mass model. However, hand calculation gives us a quick estimation and help guide us in the device design optimization. In the second vibrational mode (see Fig. 8), the mirror plates rotate along the axis of the torsional beam with resonant frequency of f_0=178.24kHz. This is the torsional mode of the micromirror. The other modes are higher order vibrational modes and they are far away from the working modes of the micromirror. As a result, they are not easily coupled into the working modes of the micromirror. This indicates that the micromirror can work stably in its working modes without interference from the higher vibrational modes.

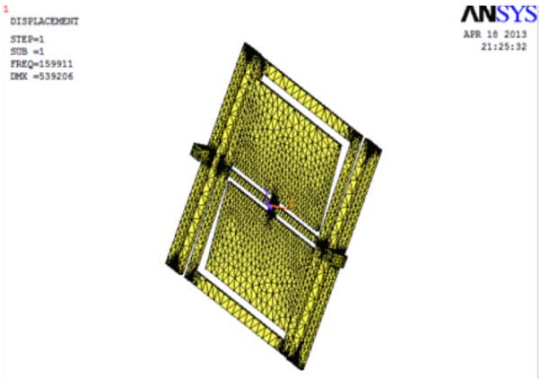

Figure 7. ANSYS simulation results of piston vibrational mode of micromirror (f_0=159.91kHz)

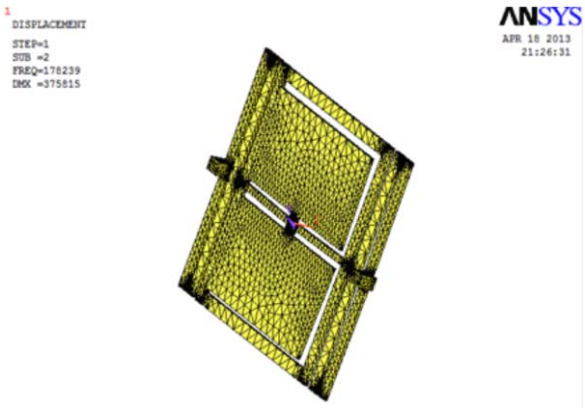

Figure 8. ANSYS simulation results of torsional vibrational mode of micromirror (f0=178.24kHz)

The proposed micromirror is to be fabricated with surface-micromachining using thick photoresist sacrificial layer technique [11].

V. CONCLUSIONS AND FUTURE WORK

In this paper, a surface-micromachined MEMS dual-mode micromirror is proposed. The micromirror utilizes folded beams for its piston mode and two straight torsional beams for its torsional mode. By controlling two switches connected to bottom aluminum electrodes, the micromirror can be activated to work in either piston or torsional mode. It combines both functions into a single device, leading to improved functionality and more flexibility. A theoretical model is used to analyze the performance of the micromirror, and equations are derived to predict its behavior in both piston and torsional modes. ANSYS modal simulation is used to analyze the dynamic behavior of the micromirror. The resonant frequencies of both working modes are extracted. The micromirror can be used for light display, optical communication and other applications.

In the future, we will further improve the design of the proposed dual-mode micromirror, so that the mirror structure is more stable and the coupling effects between the piston and torsional modes can be minimized. For example, another dual-mode micromirror design is shown in Fig. 9, with the torsional beams in parallel with the folded beams. Since the torsional beams are perpendicular to the axis of the connectors of folded beams, this may reduce the coupling of tilting of folded beams to the torsinal rotation of mirror plates in torsional mode.

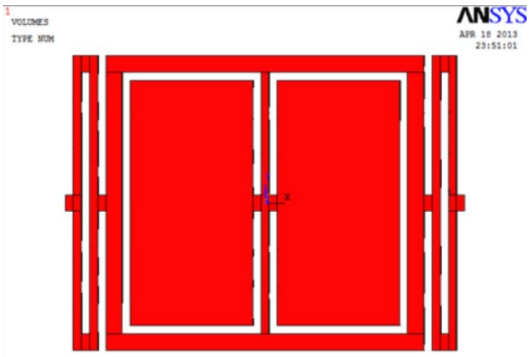

Figure 9. ANSYS model of improved design #1: torsional mirror parallel to folded beams

We are also considering an improved mirror structure design as shown in Fig. 10. In it, the mirror frame is connected to 8 sets of folded beams in it all four directions. This makes the mirror frame more stable and further reduces the coupling of rotation of folded beams into the torsional mode of the micromirror. A thorough analysis and ANSYS simulation are needed to compare these improved designs with the original design.

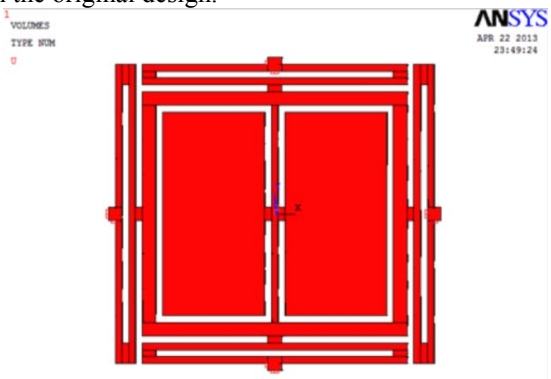

Figure 10. ANSYS model of improved design #2: mirror frames connected to folded beams in all 4 directions

REFERENCES

[1] D.W. Monk, "Digital light processing: a new image technology for the television of the future", 1997 International Broadcasting Convention, Sept. 12-16, 1997, pp. 581-586.

[2] I.W. Jung, U. Krishnamoorthy, O. Solgaard, "High fill-factor two-axis gimbaled tip-tilt-piston micromirror array actuated by self-Aligned vertical electrostatic combdrives", Journal of Microelectromechanical Systems, Vol. 15, Issue 3, June 2006, pp. 563-571.

[3] A. Werber, H. Zappe, "A thermo-pneumatically actuated tip-tilt-piston mirror", 2007 IEEE/LEOS International Conference on Optical MEMS and Nanophotonics, July 16 - Aug. 12, 2007, pp. 47-48.

[4] K.B. Lee, L. Lin, "A vertically-supported two-axial torsional micromirror", *Micro Electro Mechanical Systems, 2004. 17th IEEE International Conference on. MEMS*, pp. 41-44.

[5] S. Zairi, G.Y. Tian, "Design of buried hinge based 3D torsional micro mirrors", *High Density Microsystem Design and Packaging and Component Failure Analysis, 2004. HDP '04. Proceeding of the Sixth IEEE CPMT Conference on.*, pp. 164-170.

[6] V. Milanovic, S. Kwon, L.P. Lee, "High aspect ratio micromirrors with large static rotation and piston actuation", *IEEE Photonics Technology Letters*, Vol. 16, Issue 8, 2004, pp. 1891-1893.

[7] S. W. Chung, Y. K. Kim, "Design and fabrication of 10×10 micro-spatial light modulator array for phase and amplitude modulation," in *Sensors and Actuators A: Physical,* vol. 78, pp. 63-70, 1999.

[8] U. Krishnamoorthy, K. Li, K. Yu, D. Lee, J. P. Heritage, and O. Solgaard, "Dual-mode micromirrors for optical phased array applilcations," in *Senosrs and Actuators A: Physical,* vol. 97-98, pp. 21-26, 2002.

[9] S. Yamashita, M. Mita, H. Fujita, T. Yamamoto, M. Kawai, M. Yano, "Novel spatial light phase modulator with bidirectional tilt-piston micromirror array", *2007 International Solid-State Sensors, Actuators and Microsystems Conference, TRANSDUCERS 2007*, pp. 1521-1524.

[10] A. Jain, S. Todd, H. Xie, "An electrothermally-actuated, dual-mode micromirror for large bi-directional scanning", in *2004 IEEE International Electron Devices Meeting (IEDM'04)*, Dec. 13-15, 2004, pp. 47-50.

[11] X. Xiong, T. Dallas, S. Gangopadhyay, J. Berg, T. Henryk, "Design and Simulation of Aluminum Bi-functional Spatial Light Modulator", *Proc. of the 48th IEEE International Midwest Symposium on Circuits & Systems (MWSCAS'05)*, Cincinnati, Ohio, USA, Aug 7-10, 2005, pp. 159-162.

[12] L.F. Mondolfo, Aluminum Alloys: Structure and Properties, Boston: Butterworths, 1976, pp. 108-111.

[13] X. M. Zhang, F. S. Chau, C. Quan, Y. L. Lam, and A. Q. Liu, "A study of the static characteristics of a torsional micromirror," in *Sensors and Actuators A: Physical*, vol. 2883, pp. 1-9, 2001.